

Evidence for Heme–Heme Excitonic Coupling in the Soret Circular Dichroism of Hemoglobin

Robert A. Goldbeck,¹ Laura Sagle, Daniel B. Kim-Shapiro,² Veronica Flores, and David S. Kliger
Department of Chemistry and Biochemistry, University of California, Santa Cruz, California 95064

Received May 13, 1997

In order to study interdimer heme–heme electronic interactions in human hemoglobin, the Soret circular dichroism spectrum of the carboxy adduct is measured as a function of protein concentration, the spectrum at the highest concentration representing primarily that of $\alpha_2\beta_2$ tetramers (93%) and the lowest concentration representing primarily $\alpha\beta$ dimers (68%). The tetramer–dimer difference spectrum, obtained using singular value decomposition and linear least squares fitting from a matrix of CD spectra measured at ten concentrations, is roughly conservative, with a larger negative lobe at shorter wavelengths and a peak-to-trough magnitude that is 18% of the tetramer's maximum Soret CD magnitude. It is tentatively assigned to heme-heme excitonic interactions on the basis of theoretical predictions by R. W. Woody [(1985) *in Optical Properties and Structure of Tetrapyrroles* (Blauer, G., and Sund, H., Eds.), pp. 239–256, Walter de Gruyter, New York]. © 1997 Academic Press

Interest in the origin of induced CD in heme proteins has been rekindled by recent results suggesting that mechanisms besides the electronic coupling between aromatic residues and the heme chromophore may be important in inducing optical activity in the heme absorption bands. The generally accepted mechanism for the generation of Soret band optical activity, based on Hsu and Woody's theoretical results for hemoglobin and myoglobin (1), is a coupled oscillator interaction between the heme transitions and allowed $\pi\pi^*$ transitions on nearby aromatic residues. However, this interaction cannot be the whole story in heme proteins. For instance, it is known that the Soret CD of the heme undecapeptide of horse heart cytochrome *c* is similar in magnitude to the Soret CD of other heme proteins

despite the absence of aromatic amino acid residues in the undecapeptide (2). The origin of induced CD in the case of the undecapeptide was recently explained by Blauer et al. (3), who concluded that coupled oscillator interactions with peptide $\pi\pi^*$ transitions and high-energy peptide and thioether sulfur transitions, as well as inherent heme chirality arising from nonplanar distortions, are the dominant mechanisms contributing to the Soret CD.

The present study uses the tetramer \rightarrow dimer dissociation reaction of hemoglobin-CO to examine the importance of another possible mechanism, heme to heme interactions, in inducing CD in the Soret band of hemoglobin. Induced heme band CD has been used as a probe of quaternary state in this cooperative protein in equilibrium (4) and time-resolved CD and ORD studies (5, 6) of the allosteric R \rightarrow T transition. In this regard, a coupled oscillator interaction between hemes, i.e. excitonic coupling, is an additional mechanism for the induction of Soret CD that could reflect information about changes in quaternary structure in multiheme proteins such as hemoglobin. In particular, the R \rightarrow T quaternary transition in hemoglobin produces changes in the relative distances and orientations of the hemes during the allosteric transition that could modulate the Soret CD through an excitonic mechanism. Although theoretical calculations by Woody (7) suggest that excitonic coupling makes an appreciable contribution to the Soret CD of the hemoglobin tetramer, experimental evidence for this effect has heretofore been lacking. The present study presents Soret spectral evidence for such heme-heme coupling in hemoglobin. Specifically, we find a tetramer-dimer CD difference spectrum that is consistent with excitonic coupling across dimers within the tetramer and that is comparable in magnitude to theoretically predicted values (7).

MATERIALS AND METHODS

Human hemoglobin was prepared from freshly drawn blood using the method of Geraci and Li (8) and pelleted in liquid nitrogen for later use. Pellets were dissolved in CO saturated, pH 7.3, 0.1 M

¹ To whom correspondence should be addressed. Fax: 408-459-2935. E-mail: goldbeck@chemistry.ucsc.edu.

² Present address: Department of Physics, Wake Forest University, Winston-Salem, North Carolina 27109-7507.

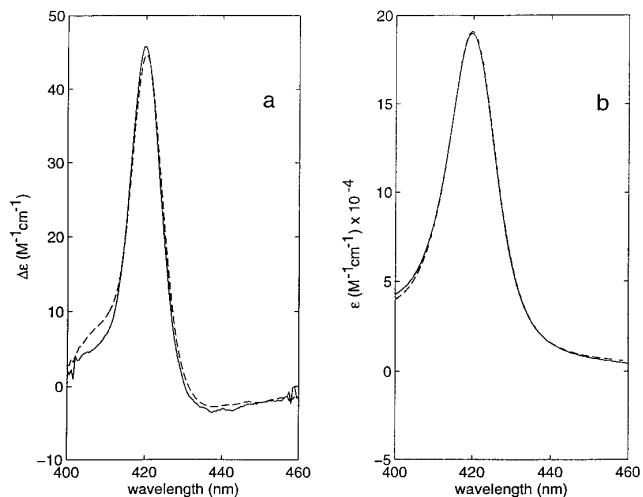


FIG. 1. (a) The Soret region CD spectrum of Hb-CO at low and high concentrations, 0.68 μM (—) and 177 μM (---) on a per heme basis. (b) Absorption spectra at the same concentrations.

sodium phosphate buffer, reduced with several drops of 0.5 M sodium dithionite solution, and placed under 1 atm CO for 45 minutes. Sample concentrations were adjusted to ten values over the range 0.7 to 180 μM , as estimated by α band absorbance (all concentrations on a per heme basis). Spectral measurements were made in airtight CD cells with path lengths of 0.5, 2, 10, and 50 mm, as appropriate for each concentration. CD spectra were recorded on an Aviv 60DS

scanning CD spectrophotometer, using a 0.5-nm bandwidth, a 5-s averaging time, and a wavelength step size of 0.5 nm. The CD spectrum reported for each concentration is the average of 120 wavelength scans. Absorption spectra were recorded on a Shimadzu UV-2101PC spectrophotometer, referenced to air. Each CD spectrum was baseline adjusted by adding an offset such that each spectrum had the same average CD over the spectral range 450-460 nm and the sum of the offsets was zero. Baseline offsets in the raw absorption spectra, mainly caused by light scattering, were determined and subtracted by means of a nonlinear simplex fitting algorithm; the raw absorption spectra were fit to the expression

$$\mathbf{A}_{\text{raw},i} = \sum_j C_j z_j \epsilon(\lambda) + b_i \quad (1)$$

where the concentrations, C_j , the extinctions, $\epsilon(\lambda)$, and the offsets, b_i , are floating parameters and the z_j are the given pathlengths. After convergence to a self-consistent set of parameters, the b_i were subtracted from the raw spectra. The concentration values used to analyze the CD data were then obtained from the baseline adjusted absorption spectra, using the literature molar extinction value of $\epsilon(419 \text{ nm}) = 191 \text{ mM}^{-1}\text{cm}^{-1}$ (9). This procedure gave the lowest heme concentration as 0.68 μM and the highest as 177 μM .

Singular value decomposition (SVD) analysis was applied to the matrices of (baseline adjusted) spectra versus concentration obtained from the CD and absorption measurements. SVD factors a data matrix \mathbf{A} as

$$\mathbf{A} = \mathbf{U}\mathbf{S}\mathbf{V}^T \quad (2)$$

where \mathbf{S} is a diagonal matrix of nonnegative elements (singular values) and \mathbf{U} and \mathbf{V} are orthonormal matrices (10). The utility of this

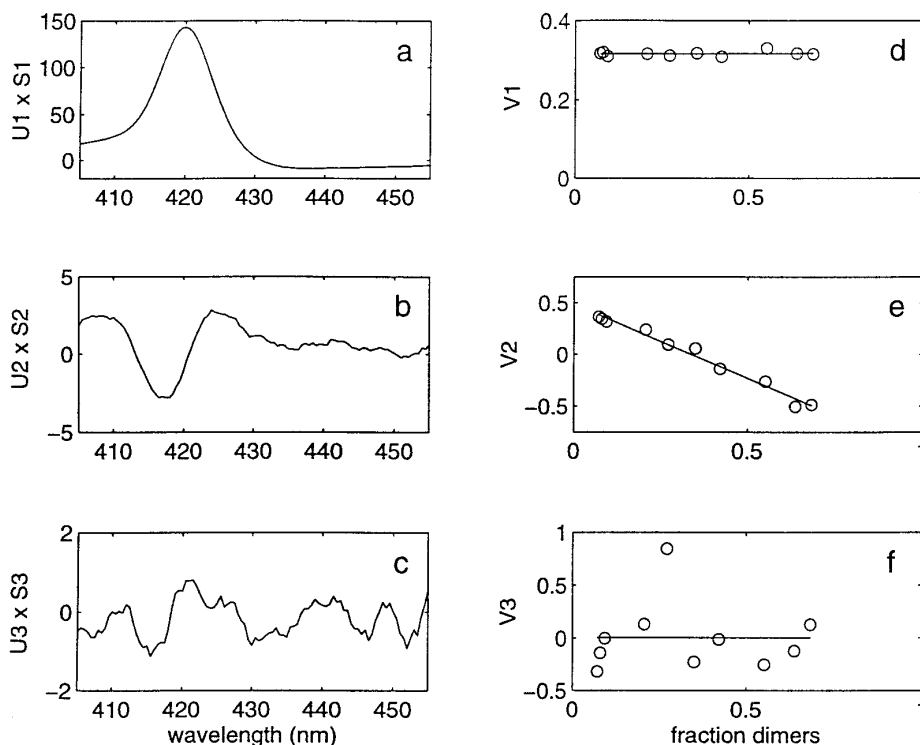


FIG. 2. SVD analysis of CD spectra measured at ten concentrations ranging from 0.68 to 177 μM (see Eq. 2). The basis spectra U_i are shown scaled by their singular values $S_{i,i}$. The elements of the orthonormal vectors V_i are proportional to the concentration dependences of the U_i spectra. (a) U_1 , (b) U_2 , (c) U_3 , (d) V_1 , (e) V_2 , and (f) V_3 . The lines in (d), (e), and (f) are linear least squares fits to the points.

procedure in the present case is the ability to discern the number of independent spectrochemical processes sensitive to heme concentration (from the number of singular values larger than a threshold noise value) and to obtain their spectral shapes (columns of \mathbf{U}) and concentration dependences (columns of \mathbf{V}), albeit in a possibly convoluted form. Spectrochemically independent processes are mixed in \mathbf{U} and \mathbf{V} by the orthonormality constraint and further analysis requires additional physicochemical assumptions. We assumed that the spectrum at each concentration C_i is given by

$$\mathbf{A}_i(\lambda) = D(\lambda) + f_i[T(\lambda) - D(\lambda)] \quad (3)$$

where $D(\lambda)$ and $T(\lambda)$ are the dimer and tetramer spectra, respectively, and f_i is the mole fraction of tetramers. The tetramer fraction was calculated from heme concentration using

$$f_i = 1 - K_d / (1 + 4C_i / K_d)^{1/2} - 1 / 2C_i \quad (4)$$

where K_d , the tetramer dissociation constant, is taken to be 1.0 μM (11). The calculated dimer fraction ($1 - f_i$) ranged from 0.68 at the lowest heme concentration to 0.07 at the highest. A linear least squares procedure was applied to Eq. 3 at each wavelength to determine the best values of $D(\lambda)$ and the difference spectrum $[T(\lambda) - D(\lambda)]$.

RESULTS AND DISCUSSION

CD and absorption spectra measured in hemoglobin-CO solutions with low and high concentrations, dominated by $\alpha\beta$ dimers and $\alpha_2\beta_2$ tetramers, respectively, are shown in Figure 1. At both concentrations, the Soret CD spectrum consists of a single positive peak, narrower in bandshape than the corresponding peak in the absorption spectrum and slightly shifted in wavelength, and a shallow negative trough at the long wavelength side of the peak. The spectral differences associated with concentration are small, which may explain why they were overlooked in previous studies (12–14), although they are more evident in the CD than in the absorption spectra. The high concentration CD spectrum is red shifted from the low concentration spectrum by less than a nanometer, a shift that is evidently associated with the increased fraction of tetramers present at high concentrations.

The effects of concentration on spectra are highlighted in the SVD analyses of the CD and absorption spectra measured at ten concentrations, shown in Figures 2 and 3, respectively. The first basis spectrum, U_1 , obtained from an SVD analysis of CD or absorption is just the concentration averaged spectrum of Hb-CO, to a good approximation. Thus Figures 2a and 3a are closely similar to Figures 1a and 1b, respectively (after scaling the former by the appropriate element of V_1 , see Eq. 2). The flat V_1 vector in Figure 2d reflects the lack of significant concentration dependence in the overall CD intensity. (Figure 3d is flat by construction because the absorption intensities were used to calculate concentrations.) The spectral variations of interest appear mostly in the second basis spectra, U_2 , which are roughly the spectral differences between high and

low concentrations and thus mainly a reflection of the tetramer–dimer difference spectra. The CD basis spectrum (Figure 2b) shows a derivative shaped exciton-like band centered near the absorption maximum at 419 nm, with an additional positive feature lying to the short wavelength side of the Soret band. The concentration dependence of the exciton-like contribution (Figure 2e) shows a negative, closely linear correlation with the fraction of dimers. The corresponding absorption basis spectrum (Figure 3b) shows a feature appearing on the long wavelength side of the absorption peak that is also suggestive of an exciton band, but its concentration dependence (Figure 3e) is much more scattered than that for the exciton-like feature in the CD. The third SVD basis spectra are essentially uncorrelated with concentration (Figures 2f and 3f) and appear to reflect mainly shot noise in the CD (Figure 2c) and instrumental artifacts in the absorption spectra (Figure 3c).

Pure dimer and tetramer CD spectra and the tetramer–dimer difference spectrum were calculated from the ten concentration-dependent spectra using Eq. (3) and are shown in Figure 4. The tetramer–dimer difference is very similar to the exciton-like feature found in the SVD analysis (Figure 2b), as expected. The peak-to-trough magnitude of the bisignate feature centered near 419 nm in Figure 4 is 18% of the peak magnitude of the tetramer CD. It is clear that the appearance of this feature in the tetramer is associated with dimer-dimer interactions within the tetramer. We propose that heme-heme couplings between dimers are the major component of these interactions. Woody (7) has calculated heme-heme electronic interaction contributions to the Soret CD of hemoglobin and the hemoglobin- O_2 complex using exciton and polarizability theories. The predictions from both methods are qualitatively similar in sign, bandshape, and magnitude for Hb with and without oxygen ligation, aside from the usual ligand-induced blue shift in wavelength, and thus are usefully compared here to the CD of the CO complex. The sign of these predictions, positive lobe at longer wavelengths, is in agreement with the effect observed here. The predicted peak-to-trough magnitudes vary from 60% of the tetramer maximum for HbO_2 to 20% (polarizability) and 10% (exciton) for Hb, the predictions for the latter being more sensitive to the theoretical model used. (The smaller relative magnitude in Hb is partly attributed to the greater average heme-heme distance in Hb compared with HbO_2 .) The predicted magnitudes are in good agreement with our observed magnitude given that total heme-heme interactions were calculated whereas our magnitude is assigned to the tetramer–dimer interaction difference, which is expected to be smaller than the total. Two of the six heme-heme interactions possible in the tetramer are already present in the dimers, and the crystal structure of Hb suggests that the heme-heme pairings within dimers may be best oriented for excitonic CD (15).

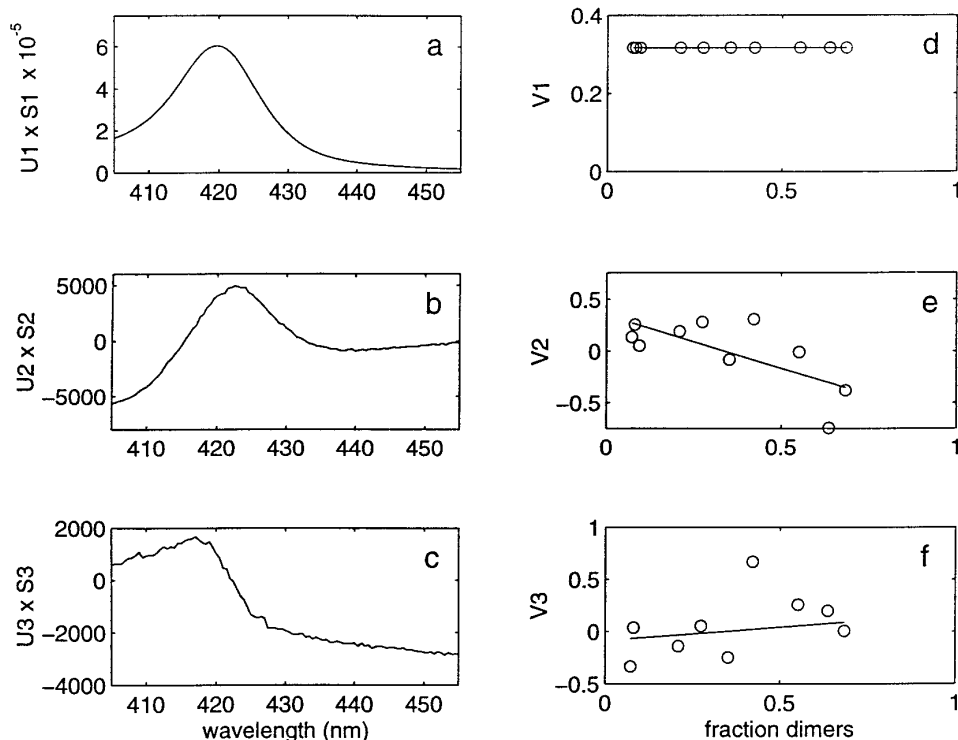


FIG. 3. SVD analysis of absorption spectra. Concentrations and labels are given in Figure 2 caption.

Some change in protein conformation could be expected to accompany association of the dimers and this may influence the tetramer–dimer difference spectrum reported here. However, the free energy of binding of R-state dimers (about 8 Kcal/mole) is relatively small (16) and consequently the effect of association on protein tertiary structure around the heme appears to be

very small. Ligand affinities and binding rate constants are sufficiently similar for R-state hemes in tetramers and dissociated dimers that studies finding small differences in these quantities between dimers and tetramers, implying significant differences in protein conformation, tend to be controversial (17, 18). In any event, the derivative shaped tetramer–dimer CD difference feature cannot arise from a conformational perturbation that simply red shifts the transition energy upon dimer binding because such a feature would also be seen in the absorption difference spectrum, contrary to observation. We cannot rule out the possibility that a change in protein conformation or distant heme-aromatic residue interactions occurring upon dimer association coincidentally produce the excitonic-like feature observed in the tetramer–dimer CD spectrum, but there is wide evidence suggesting that the first effect is very small and the second effect, across-dimer heme-aromatic electronic interactions, is expected to be small because of the poor match between transition energies. Thus, the heme-heme excitonic interaction predicted by Woody is the most compelling explanation for our observations.

ACKNOWLEDGMENTS

This work was supported by the National Institute of General Medical Sciences, Grant GM35158 (D.S.K.) and by NIH Fellowship HL0896901 to D.B.K.-S. V.F. acknowledges the support of NSF Research Experiences for Undergraduates Grant CHE-9322464.

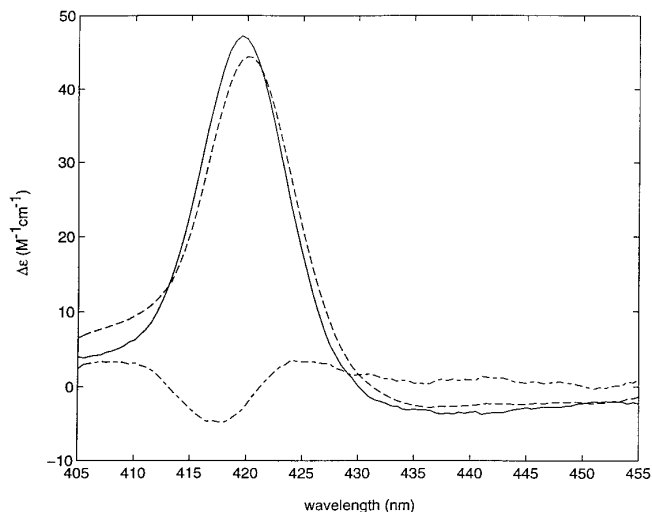


FIG. 4. The CD spectra of HbCO dimers (—) and tetramers (---), and the tetramer–dimer difference spectrum (----), calculated from Eq. (3).

REFERENCES

1. Hsu, M.-C., and Woody, R. W. (1971) *J. Am. Chem. Soc.* **93**, 3515–3525.
2. Urry, D. W. (1967) *J. Am. Chem. Soc.* **89**, 4190–4196.
3. Blauer, G., Sreerama, N., and Woody, R. W. (1993) *Biochemistry* **32**, 6674–6679.
4. Woody, R. (1978) in *Biochemical and Clinical Aspects of Hemoglobin Abnormalities* (Caughey, W. S., Ed.), pp. 279–298, Academic Press, San Diego, CA.
5. Björling, S. C., Goldbeck, R. A., Paquette, S. J., Milder, S. J., and Kliger, D. S. (1996) *Biochemistry* **35**, 8619–8627.
6. Shapiro, D. B., Goldbeck, R. A., Che, D., Esquerra, R. M., Paquette, S. J., and Kliger, D. S. (1995) *Biophys. J.* **68**, 326–334.
7. Woody, R. W. (1985) in *Optical Properties and Structure of Tetrapyrroles* (Blauer, G. and Sund, H., Eds.), pp. 239–256, Walter de Gruyter, New York, NY.
8. Geraci, G., and Li, T.-K. (1969) *Biochemistry* **8**, 1848–1854.
9. Antonini, E., and Brunori, M. (1971) *Hemoglobin and Myoglobin in Their Reactions with Ligands*, p. 19, Elsevier, New York.
10. Hendler, R. W., and Shrager, R. I. (1994) *J. Biochem. Biophys. Methods* **28**, 1–33.
11. Chu, A. H., and Ackers, G. K. (1981) *J. Biol. Chem.* **256**, 1199–1205.
12. Brunori, M., Engel, J., and Schuster, T. M. (1967) *J. Biol. Chem.* **242**, 773–776.
13. Geraci, G., and Li, T.-K. (1969) *Biochemistry* **8**, 1848–1854.
14. Mawatari, K., Matsukawa, S., and Yoneyama, Y. (1983) *Biochim. Biophys. Acta* **745**, 219–228.
15. Dickerson, R. E., and Geis, I. (1983) *Hemoglobin: Structure, Function, Evolution, and Pathology*, Benjamin/Cummings, Menlo Park, CA.
16. Turner, B. W., Pettigrew, D. W., and Ackers, G. K. (1981) *Methods Enzymol.* **76**, 596–628.
17. Ackers, G. K., and Johnson, M. L. (1990) *Biophys. Chem.* **37**, 265–279.
18. Ghelichkhani, E., Goldbeck, R. A., Lewis, J. W., and Kliger, D. S. (1996) *Biophys. J.* **71**, 1596–1604.